



RESEARCH ARTICLE

Optimization of Slag Content and Properties Improvement of Metakaolin-slag Geopolymer Mixes

M. F. Zawrah*, R. A. Gado and R. M. Khattab

National Research Centre, Ceramics Department-Center of Excellence for Advanced Sciences, 12622-Dokki, Cairo, Egypt

Received: April 4, 2018

Revised: June 12, 2018

Accepted: June 20, 2018

Abstract:

Object:

Geopolymers mixes were fabricated from Metakaolin (MK) and Blast Furnace Slag (BFS) waste material in the presence of sodium hydroxide and sodium silicate which were used as alkali activators. To optimize the suitable amount of slag, eleven batches were designed, mixed and homogenized for 30 min.

Method:

To determine the suitable amount of liquid required for pasting, normal consistency and setting time were determined. The physico-mechanical properties at different curing ages *i.e.* 3, 7, 28 and 90 days, were determined. X-ray diffraction and scanning electron microscope were used to investigate phase composition and microstructure.

Result:

To guarantee forming geopolymer gel and to check its amount, HCl extraction test was performed. Salicylic acid/methanol extraction was also performed to verify the presence and amount of Calcium Silicate Hydrate (CSH). The results revealed that calcium-rich slag (BFS) accelerated the hardening process and decreased the alkaline liquid consistency. For geopolymer without BFS, two phases, namely; un-reacted metakaolin and geopolymer gel were formed. For geopolymers with BFS, three phases were formed, namely; un-reacted metakaolin, geopolymer gel and CSH with aluminum substitution (CASH) gel. The bulk density was increased with increasing BFS and curing time. The strength was increased with increasing of BFS, reaching its maximum (about 120 MPa) for the specimen containing 70% slag, cured for 28 days.

Keywords: Geopolymer, Metakaolin, Slag, Properties, Calcium Silicate Hydrate (CSH), X-ray.

1. INTRODUCTION

Recently, new type of un-fired ceramic materials has received attention. This material often refers to geopolymer or inorganic polymer. At the end of 1970s, geopolymer has been identified and used by J. Davidovits. Recently, geopolymer known as alkali activated aluminosilicate binders with the general formula $M_2O.mAl_2O_3.nSiO_2$, where $m \approx 1$ and $2 \leq n \leq 6$ (M usually is Na or K) [1]. It forms by the reaction of an aluminosilicate material with highly concentrated alkaline solution [2]. The presence of higher amounts of Al and Si causes re-condensation of soluble ions which consequently assemble into inorganic polymer and create amorphous network with high mechanical strength compared with other binding materials. In this polymerization process, water doesn't consume for hydration; it has an active role as a dissolution medium. The alkali ions in the medium are connected in geopolymer network through balancing with Al and Si [3].

* Address for correspondence to this author at the National Research Centre, Ceramics Department-Center of Excellence for Advanced Sciences, 12622-Dokki, Cairo, Egypt, Tel: +201222437949, Fax: +20233370931; E-mail: mzawrah@hotmail.com

Generally, geopolymer can be prepared at ambient or elevated temperature using aluminosilicates. There are many sources of geopolymer starting materials to be used mixed or as individuals; such as waste materials, kaolin, pozzolanic materials, melt quenched aluminum silicates and volcanic scoria [4 - 8]. It has several important applications as binding materials, advanced ceramics, fire retardant materials, high technological materials, and stabilizer for hazardous materials [9].

Geopolymerization proceeds through dissolution, polymerization, reorganization and hardening [10]. In highly concentrated alkaline aqueous solution, aluminum silicates are quickly dissolved to form free SiO_4 and AlO_4 tetrahedral units freely distributed in the medium. During progressing of reaction, H_2O comes apart and the formed tetrahedral units are connected alternatively by sharing all oxygen atoms to give three kinds of geopolymers; (a) poly-sialate [$-\text{SiO}_4-\text{AlO}_4-$] (PS type), (b) poly-sialate-siloxo [$-\text{SiO}_4-\text{AlO}_4-\text{SiO}_4-$] (PSS type), or (c) polysialate-disiloxo [$-\text{SiO}_4-\text{AlO}_4-\text{SiO}_4-\text{SiO}_4-$] (PSDS type). This means that Si:Al ratios in the three types are Si:Al=1 for sialate ($-\text{Si}-\text{O}-\text{Al}-\text{O}-$), Si:Al=2 for sialate siloxo ($-\text{Si}-\text{O}-\text{Si}-\text{Al}-\text{O}-$), Si:Al=3 for sialate-disiloxo ($-\text{Si}-\text{O}-\text{Al}-\text{O}-\text{Si}-\text{O}-\text{Si}-$) and Si:Al>3 when it is poly (sialate-multisiloxo) [11]. After hardening, the materials have excellent compressive strength, compactness, durability and anticorrosion [12]. There are many natural or waste sources such as fly ash and blast furnace slag that contain calcium ions and can be used in geopolymer fabrication. Calcium can play important role in geopolymer; it can make the system to undergo two separate and competing reactions. The first one is the formation of geopolymer while the second is the formation of calcium silicate hydrate or calcium aluminum silicate hydrate (CASH). This means that the presence of calcium raises the strength of geopolymer cured at ambient condition, while it decreases the strength of geopolymer treated at elevated temperature. This is due to that the presence of calcium hinders the formation of 3D network structure in geopolymer gel [13, 14]. However, previous study reported the presence of both calcium silicate hydrate and geopolymer gel in the matrix have valuable effects on the mechanical properties since it acts as micro-aggregates in geopolymer gel and forms a denser and more uniform binder [15].

In comparison with normal cement, geopolymer has lower energy consumption and CO_2 emission, good physico-mechanical properties as strength, shrinkage, permeability, durability, and has good resistance for fire and acids [16, 17].

Blast furnace slag is a by-product material produced from iron blast furnace after quenching in water or air. It composed mainly from $\text{CaO}-\text{SiO}_2-\text{MgO}-\text{Al}_2\text{O}_3$ oxides and can form the mixture of following phases: gehlenite ($2\text{CaO}.\text{Al}_2\text{O}_3.\text{SiO}_2$) and akermanite ($2\text{CaO}.\text{MgO}.2\text{SiO}_2$), and de-polymerized calcium aluminum silicate glass. Previous study by Yip *et al.* reported the influence of slag addition on metakaolin geopolymer [18].

The purpose of this article is to study the influence of BFS addition (up to 100%) on geopolymerization reaction of metakaolin-based geopolymer at room temperature. The optimum amount of slag to give improved properties was identified. The produced geopolymers were investigated for their physico-mechanical properties, salicylic acid/methanol (SAM) extraction, hydrochloric acid (HCl) extraction, X-ray diffraction, FTIR and SEM.

2. EXPERIMENTAL METHODS

2.1. Starting Materials

Kaolin was supplied from general company for ceramic & porcelain products (Sheeni), Egypt. Metakaolin (MK) was prepared by calcination of kaolin at 850°C for 3 hours in a furnace with heating rate of $5^\circ\text{C}/\text{min}$ then milled in planetary ball mill for 30 min to produce MK powder having Blaine specific surface area of $2,120 \text{ m}^2/\text{kg}$ and specific gravity of $2500 \text{ kg}/\text{m}^3$. BFS used in this study, is water cooled slag supplied from Iron and Steel Factory, Helwan, Egypt. The slag was firstly ground in laboratory ball mill for 3 hours to obtain Blaine specific surface area of $610 \text{ m}^2/\text{kg}$ with specific gravity of $3000 \text{ kg}/\text{m}^3$. The chemical composition of MK and BFS was determined by X-ray fluorescence. The particle size distribution of MK and BFS was determined through laser granulometry. The mineral phases were identified by XRD using Philips D-Expert, Netherlands, diffractometer with Ni filter, Cu Ka radiation at scan speed of $0.5^\circ \text{ min}^{-1}$. FTIR was conducted for starting materials using JASCO FT/IR-6100. The spectrum was recorded between 400 and 4000 cm^{-1} with resolution of 4 cm^{-1} at 25°C .

NaOH pellet (98% purity) was supplied from Sigma. 10 molar NaOH solution was prepared and kept to cool down at room temperature before preparing of the pastes. Sodium silicate solution was purchased from Fisher scientific, UK., with chemical composition of 30.1% SiO_2 , 9.4% Na_2O and 60.5% H_2O (silicate modulus, $\text{SiO}_2/\text{Na}_2\text{O} = 3.2$), specific gravity at $20^\circ\text{C} = 1.5 \text{ g}/\text{ml}$. Alkali activator solution was prepared by mixing sodium silicate solution and NaOH (10M)

solution by 1:1 ratio, and left until clear solution obtained. This solution was prepared for minimum 24 h before preparation of pastes to allow its equilibration [19, 20].

2.2. Geopolymer Preparation

Several batches composed of metakaolin MK and BFS were designed, mixed and homogenized for 30 min by ball mill as illustrated in (Table 1).

Table 1. Designed geopolymer mixes.

Mixes	G	G ₁	G ₂	G ₃	G ₄	G ₅	G ₆	G ₇	G ₈	G ₉	G ₁₀
MK	100	90	80	70	60	50	40	30	20	10	0
GGBFS	0	10	20	30	40	50	60	70	80	90	100
Total, %	100	100	100	100	100	100	100	100	100	100	100

To determine the suitable amount of liquids needed for mixing, normal consistency and setting time were determined using Humboldt Vicat's apparatus [21, 22]. Here, alkaline solution was used instead of water. To prepare geopolymer pastes, the required alkali activator solution of predetermined normal consistency [ASTM: C 187 - 1998] was added to the mixes depending on the proportions of mixes ingredients. To ensure good adherence among mix ingredients, the mixing operation was then completed by continuous vigorous mixing for about ten minutes by hand. The fresh mixes pastes were poured in plastic cubical moulds with 25×25mm dimensions then vibrated on vibrating table for period of 1-2 minutes to remove any air bubbles to give better compacted paste. The surface of paste was smoothed by the aid of thin edged trowel. Then the mould covered by plastic thin film to prevent excessive moisture loss and kept within humidity chamber at 100% relative humidity at constant temperature of 23 ±2°C for the first 24 hours. The prepared cubes were de-molded and left at ambient temperature. All samples were cured at atmospheric pressure and no attempt was made to control the humidity during curing under ambient laboratory conditions (dry cured).

2.3. Geopolymer Characterization

Physico-mechanical properties at different curing ages *i.e.* 3, 7, 28 and 90 days were determined. Three samples of each mix were randomly selected to determine bulk density, apparent porosity, water absorption and compressive strength according to [ASTM C 20=2000] and [ASTM: C109]. Bulk density, apparent porosity and water absorption were determined by water displacement method according to Archimedes principle. The compressive strength was carried out using automatic hydraulic testing machine type SHIMADZU of maximum capacity 1000 KN by rate of 0.025 KN/mm²/s. To ensure forming geopolymer gel and to monitor the amount of formed geopolymer gel through alkaline activation, hydrochloric (HCl) acid extraction test was performed [23, 24]. Salicylic acid/methanol (SAM) extraction was also performed to verify the presence and amount of CSH. The extraction process leaves only the unreacted precursors. When these methods are performed, it is possible to determine how much geopolymer, CSH and unreacted material are present. XRD, FTIR and scanning electron microscopy (SEM-JEOL Ltd., Japan) attached with EDX unit were used to investigate phase and structure composition as well as microstructure of the obtained geopolymers.

3. RESULTS AND DISCUSSION

3.1. Starting Material Characteristics

The chemical analysis of MK and BFS analyzed by x-ray fluorescence is illustrated in Table 2. It is indicated that the main components of MK are silica and alumina. The basicity coefficient ($K_b = \text{CaO} + \text{MgO} / \text{SiO}_2 + \text{Al}_2\text{O}_3$) and the quality coefficient ($\text{CaO} + \text{MgO} + \text{Al}_2\text{O}_3 / \text{SiO}_2 + \text{TiO}_2$) calculated for BFS are 1.48 and 2.13, respectively. The particles size range of MK and BFS are $d_{50} \approx 400$ and ≈ 800 nm, respectively as shown in (Fig. 1).

Table 2. Chemical composition of starting materials.

Main Oxides	SiO ₂	Al ₂ O ₃	Fe ₂ O ₃	CaO	Na ₂ O	K ₂ O	TiO ₂	MnO	MgO	SO ₃	BaO	L.O.I
MK	46.68	35.75	1.49	0.10	0.05	2.96	0.07	0.01	0.19	0.03	0.02	12.18
GBFS	26.15	7.43	1.31	44.38	0.75	0.53	0.68	5.25	5.52	2.90	4.72	---

XRD analyses of kaolin, MK and BFS are shown in Fig. (2). It indicated that the kaolin exhibits typical diffraction pattern of well crystallized layer lattice of kaolinite with muscovite impurities (illite mineral). Transformation of kaolin to metakaolin is detected after calcination at 850°C. The calcination leads to break down of the crystal structure, producing amorphous or semi crystalline phases (silica and alumina in reactive form). The characteristic peaks for kaolinite at $2\theta=12.34, 20.34, 24.87$ and 26.40 are disappeared, while another weak peaks assigned to quartz at $2\theta =20.83$ and 26.64 ; Illite at $2\theta = 9.11$ and 15.91 remained in metakaolin pattern [25]. XRD of BFS shows halo hump between $2\theta= 20-40$, indicating the amorphous nature of material with some semi crystalline phases such as merwinite and melilite. Merwinite has the composition $2CaO.Al_2O_3.SiO_2$; while melilite is solid solution series between gehlenite ($2CaO.Al_2O_3.SiO_2$) and akermanite ($2CaO.MgO.3SiO_2$). The unusual crystallinity of slag comes always from its quenching during production. For the supplied slag in the present study, it was not rapidly quenched in water or air, but during its transportation, it was gradually cooled at ambient temperature and then quenched in water [26].

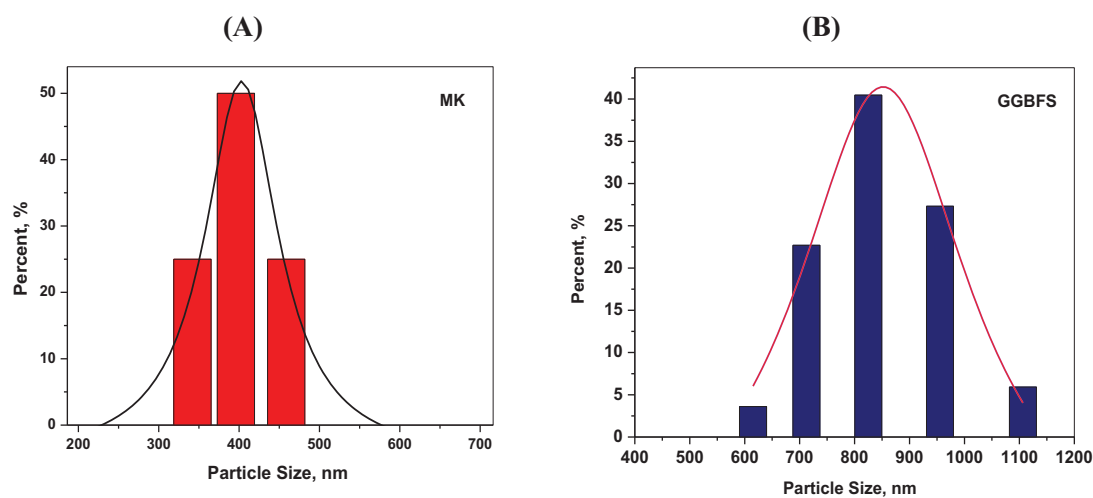


Fig. (1). Particle size distribution of Metakaolin (a) and BFS (b).

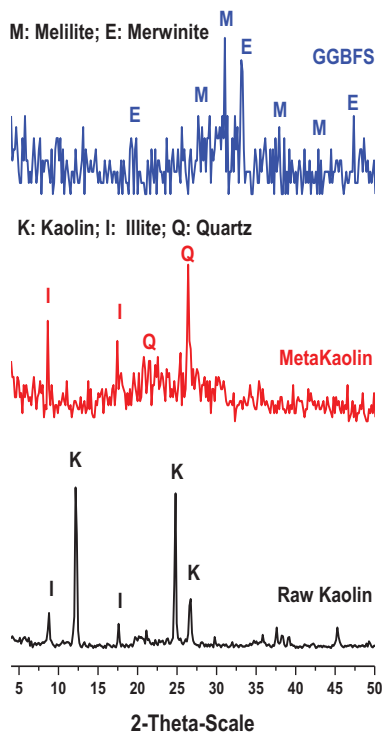


Fig. (2). XRD patterns of starting materials.

IR spectra of kaolin, MK and BFS are shown in Fig. (3). A characteristic spectrum of kaolin bands at 3695 and 3620 cm^{-1} are appeared which ascribed to the vibration of external hydroxyl and inner hydroxyl, respectively. The bands indicated at 3455 and 1630 cm^{-1} could be assigned to OH vibrational mode of hydroxyl molecule in water, which is observed in almost all natural hydrous silicates. The band at 1033 cm^{-1} is for the main functional Si-O group. Muscovite and possibly quartz interference could be observed at 1031-1038 cm^{-1} for kaolin. Al-OH peak is identified at 912 cm^{-1} . The doublet at 754-789 cm^{-1} is due to Si-O-Si inter tetrahedral bridging bonds in SiO_2 and OH deformation band. The spectra of kaolin exhibit Si-O stretching vibrations at 754, 697 and 467 cm^{-1} which are indicative of the presence of quartz [27]. The spectrum of MK exhibits main broad band at 1065 cm^{-1} which ascribed to disorder induced by dehydroxylation process of kaolin and formation of amorphous structures. Reduction in bands observed at 3433 and 1628 cm^{-1} , was assigned to the OH vibrational mode of hydroxyl molecule in water. The vibration mode at 807 cm^{-1} is associated with Al-O bonds of tetrahedral Al, while Si-O bending vibration at about 472 cm^{-1} is also detected [28].

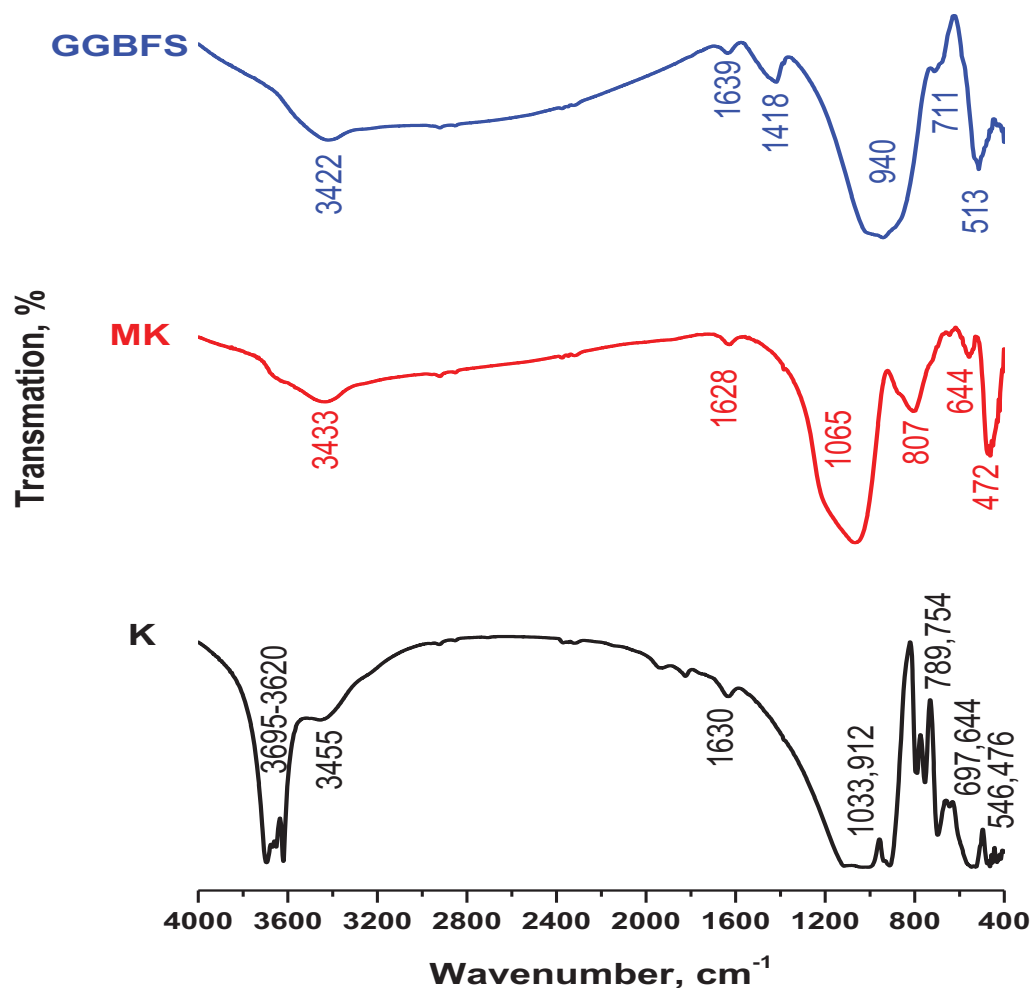


Fig. (3). FTIR of starting materials.

The spectrum of BFS shows broad vibration modes at 940 cm^{-1} which is characteristic of T-O (where T is Si or Al) bonds of tetrahedral silicates. The band at 711 cm^{-1} is attributed to the bending vibration mode of Al-O-Si bonds. These two bands are also corresponding to gehlenite [29], which has been confirmed by X-ray diffraction. The band at 1418 cm^{-1} is assigned to asymmetric vibration mode of O-C-O bonds in carbonates. This confirms the partial carbonation identified in raw material due to the weathering during storage [30].

3.2. Alkaline Liquid Consistency and Setting Time of Geopolymer Pastes

The normal consistency and setting time are important parameters in practice for cementitious material pastes for workability determination. The normal consistency determines the optimum percentage of liquid/solid ratio to form

paste suitable for shaping [31, 32]. The results of normal consistency and setting time are given in Fig. (4). The main factors affecting geopolymer setting time are chemical and phase compositions of raw materials, properties of alkaline activators, solid loading, fineness of solids and curing temperature [33 - 35]. The addition of calcium-rich BFS to MK based geopolymers causes improvement and shorting in setting time of geopolymer by forming calcium aluminum silicate hydrate (CASH) gel in addition to the sodium aluminum silicate hydrate (NASH) gel (geopolymer gel) [36, 37] with compact microstructure [38]. BFS accelerates the hardening process and decreases the alkaline liquid consistency. This is related to the formation of higher yield stress in gel structure and thus is markedly influenced by increasing the rate of crosslinking [39].

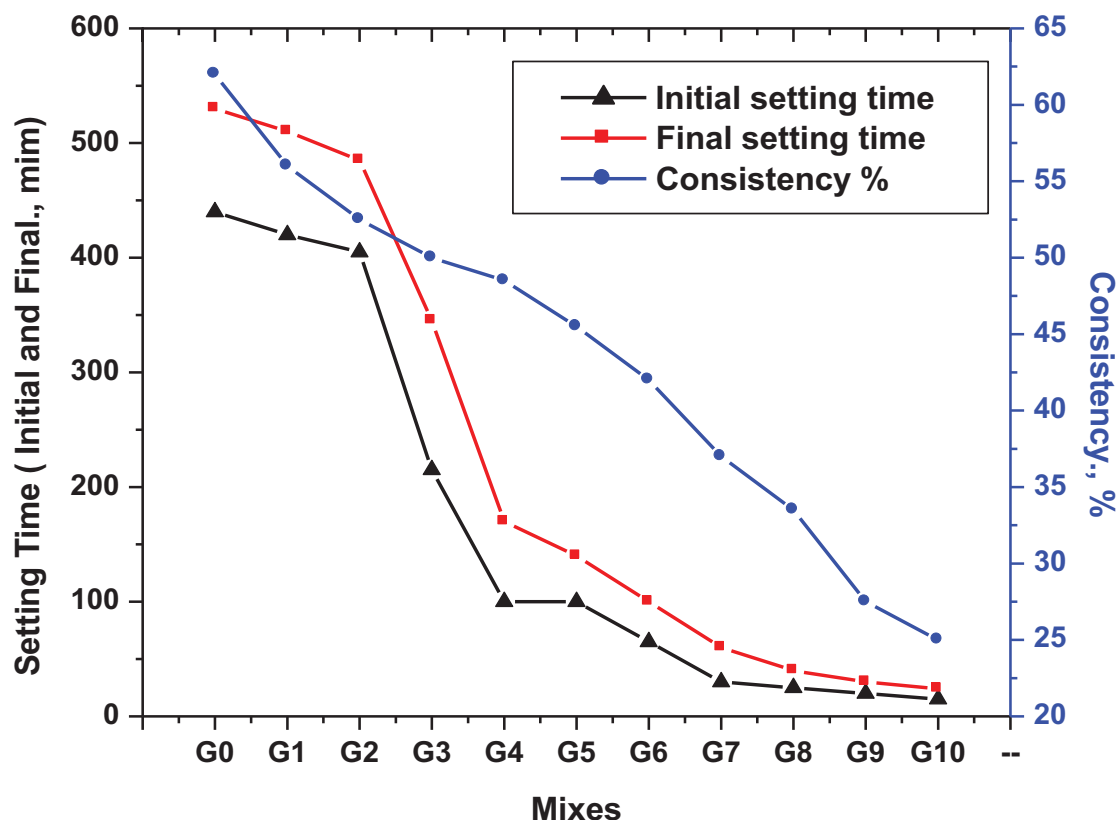


Fig. (4). Normal consistency and setting times of prepared mixes.

In metakaolin-slag geopolymer, two mechanisms have been reported for the alkali activated binding geopolymers; the first one is slag activation (Si+Ca) with gentle alkaline medium leading to CSH as the main reaction products. The second one is the alkali activation of metakaolin (Si+Al) with medium to high alkaline media. They can form zeolite like polymers (gel structure). It has been reported by Davidovits that the second groups are considered as “Geopolymer” since they have polymeric structure [40, 41].

3.3. Geopolymer Characterization

3.3.1. Physico-mechanical Properties

The physico-mechanical properties in terms of bulk density, apparent porosity, water absorption and compressive strength of metakaolin-slag geopolymers prepared at different curing ages are given in Fig. (5). As indicated, by increasing BFS content in the mixes, the bulk density increases from 1.67-2.33g/cm³ Fig. (5a). Moreover, the bulk density increases with increasing curing time. As a result of adding BFS in geopolymer system, different chemical reactions which lead to different products are occurred. This leads to different bulk density and thus higher compressive strength is achieved. On the other hand, with increasing BFS content, the porosity and water absorption are decreased as illustrated in Figs. (5b, c). This is due to the formation of CASH with geopolymer network. Moreover, the water

absorption which depends on the microstructure and porosity of the specimens is decreased with increasing curing time. Water absorption is considered as an indicator for the degree of geopolymeric reaction. The compressive strength Fig. (5d) increases with increasing slag content and curing time reaching its maximum value with batch G7 (118MPa after 28 day) after which its value decreases. The results of compressive strength after 28 days curing are relatively similar to that after 90 days curing. The strength variation implies that there are changes in gel content and reaction nature between the mixes which takes place leading to microstructural changes induced in geopolymers when BFS is substituted for metakaolin. With increasing the dosage of BFS to 80% (G8), deterioration in compressive strength is obtained. The compressive strengths of the geopolymer with 60 and 70wt.-% BFS are 93 and 118 MPa, respectively, while those with 80wt.-%, and 90 wt% are 77 and 58 MPa, respectively. The compressive strength of MK-based geopolymer is 43 MPa which is less than half that of G7; by other word, G7 exhibits approximately a tripling in compressive strength as compared with MK-based sample (G0). This is attributed to the reaction of Ca supplied by BFS with some excess to silicates present to form additional strength-giving gel *i.e.* Ca ion plays the key role in geopolymer skeleton. In fact, the high CaO content effects in quicker geopolymerization and development of semi-crystalline Ca-Al-Si hydrate gel produced from reaction between calcium silicate hydrate (CSH) and aluminosilicate group strengthen the network [42, 43].

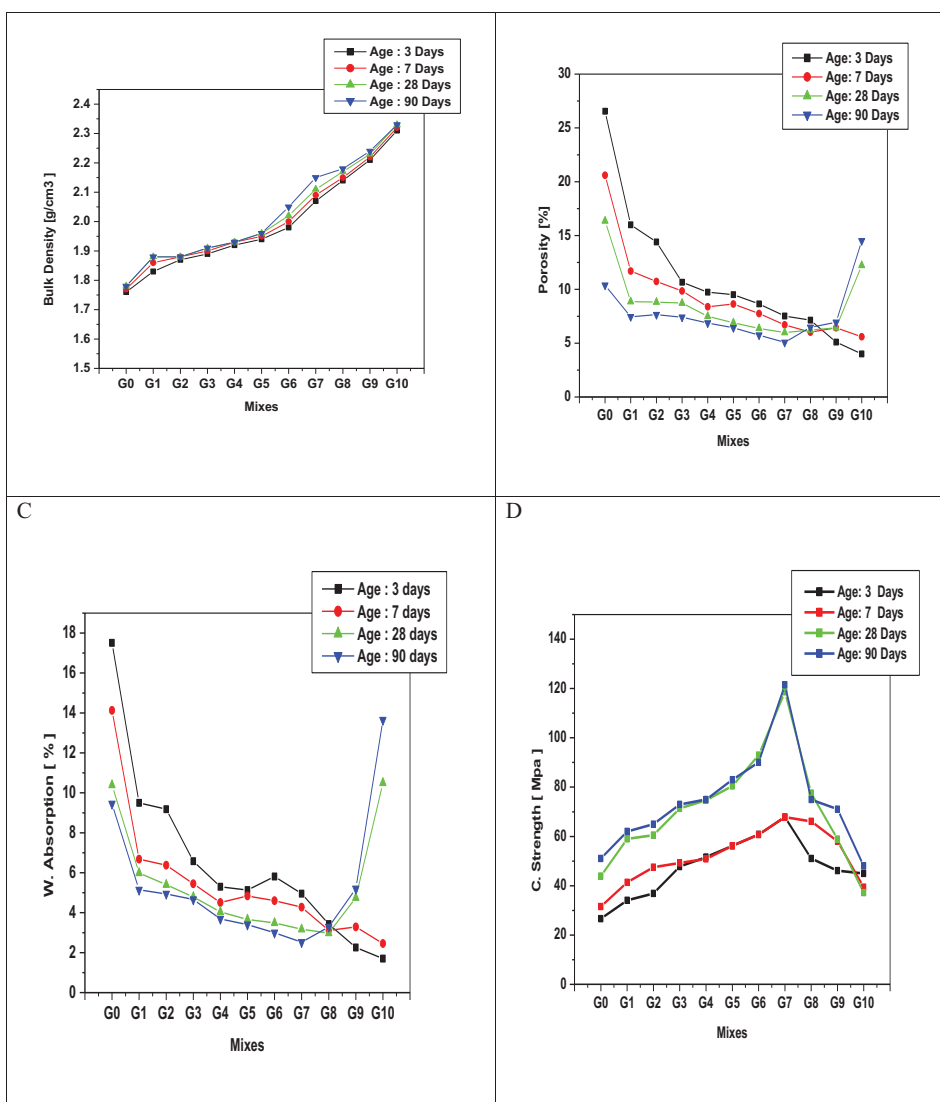


Fig. (5). Physico-mechanical properties of geopolymers.

Before testing the compressive strength, the samples were inspected visually for any potential crack. They were fairly good and no crack was observed visually for the samples G0 until G7. As seen in Fig. (6), the samples contain more than 70% BFS exhibit cracks which reflected negatively on physical and mechanical properties of specimens. This is supposed to be due to the volume changes that could happen when forming an amorphous to semi-crystalline CSH gel inside an incompletely hardened geopolymer gel.

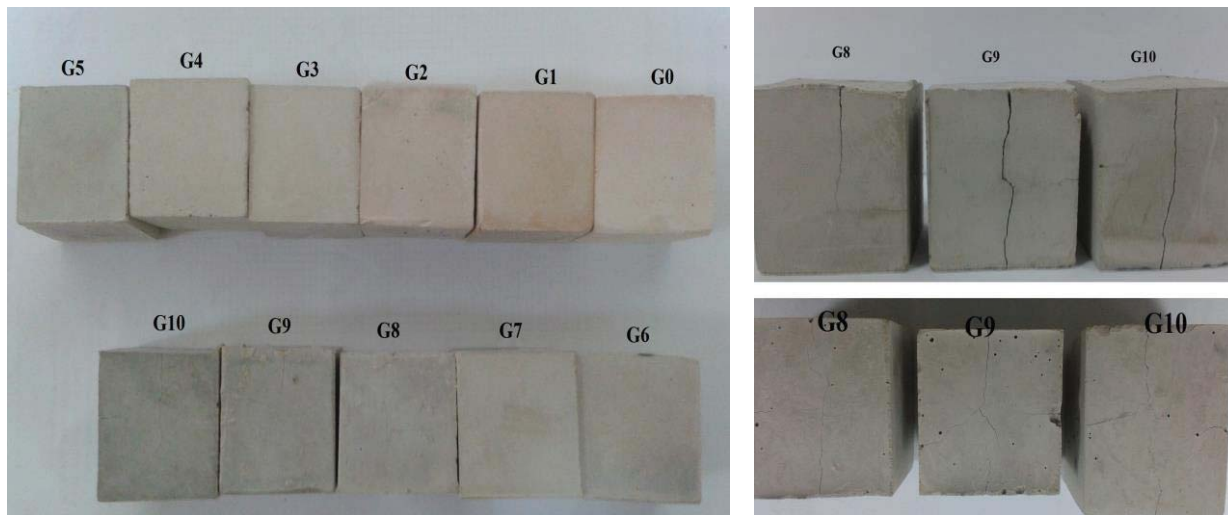


Fig. (6). Images of metakaolin-slag geopolymer specimens after curing in air.

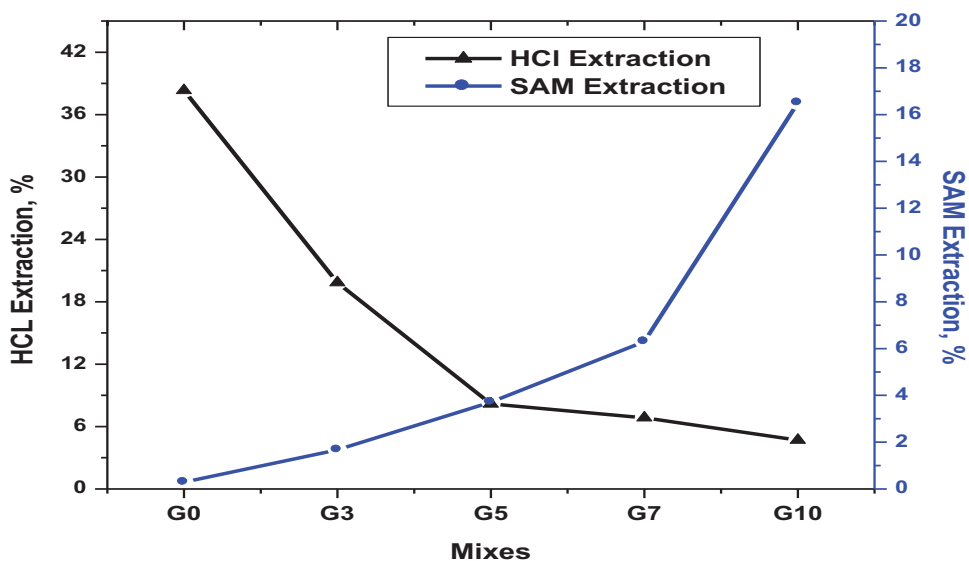


Fig. (7). HCl & SAM extractions of geopolymers.

The prepared geopolymers contain two or three phases depending on whether BFS is used or not. For geopolymer with no BFS (G0), it contains two phases, namely; un-reacted metakaolin and geopolymer gel. For geopolymers with calcium oxide sourced from BFS (G1-G10), the samples contain three phases, namely; un-reacted metakaolin, geopolymer gel and CSH with CASH [44]. Fig. (7) depicts the results of HCl and SAM extractions for G0, G3, G5, G7 and G10 geopolymers. HCl dissolves geopolymer gel and CSH reaction products and leaves un-reacted metakaolin. As shown in Fig. (7), HCl extraction results show that G0 retains more un-reacted material as compared with other geopolymers containing BFS (G1-G10). The amount of un-reacted metakaolin remained in geopolymer is 38%. This is due to incomplete geopolymerization process. The amount of un-reacted metakaolin remained after HCl extraction decreases as the BFS% increases which indicates increasing the acceleration rate of geopolymerization process. As indicated in Fig. (7), SAM extraction results show that geopolymer with 0% BFS does not have any CSH phases. The

CSH phases in matrix increases as the BFS increases which indicates the formation of new CSH phases in associated with geopolymer products as a result of the presence of CaO. The amount of CSH type phases in G10 matrix is 16% which may be due to alkali activation process for BFS only. SAM extraction results are correlated well with the result of XRD which shows low intensity for CSH phases formed in geopolymer samples G3-G7.

3.3.2. XRD of Geopolymers

XRD patterns of G, G₃, G₅, G₇ and G₁₀ geopolymers aged for 28 days are shown in Fig. (8). It worthy to mention that most of geopolymer binders produced in this study contain a very high percentage of amorphous or few semi-crystalline phases. The major phase of geopolymer samples (G-G₇) is amorphous as indicated by the broad hump at $2\theta=20-40$. The amorphous phase (Na-ASH) is obtained from dissolution of kaolinite particle in alkaline activator and then reconstruction of AlO_4 and SiO_4 species as gel structure [45, 46]. Some quartz and illite remain as crystalline phases in the geopolymers G, G₃ and G₅ [47].

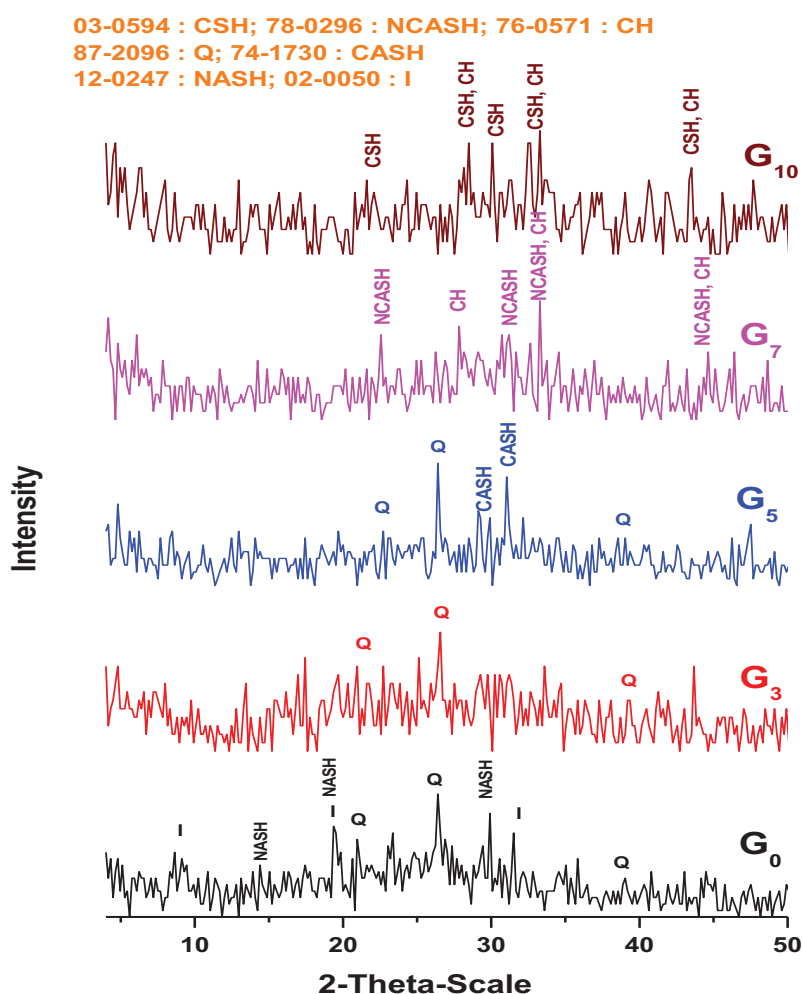


Fig. (8). XRD patterns of G, G₃, G₅, G₇ and G₁₀ geopolymers cured for 28 days.

The Na-ASH gel structure is a charge-balanced aluminum silicate influence by Si/Al ratio and alkali cations present. The mechanism of alkali-activated MK (geopolymers) involves poly condensation reaction of geopolymeric precursors *i.e.* aluminum silicate oxide with alkali poly-sialates forming polymeric Si–O–Al bond [48]. Many authors [49, 50] reported that the product of MK activation with NaOH in the presence of sodium silicate solutions is Na-ASH gel with good mechanical properties as obtained in G.

XRD patterns of G₃-G₇ have the same amorphous character as that pattern generated by G with some crystalline phase's inclusions. The alkaline activation of BFS leads to acceleration of polymerization and formation of some new phases that may help the geopolymeric gel for the development of its strength. It is well known that calcium silicate

hydrate (CSH) phases are the main binding phase in BFS alkali-activated materials having low C/S ratio with varying degrees of crystallinity [51]. The presence of CSH and geopolymer gels has been reported previously in various systems containing $\text{Ca}(\text{OH})_2$ or slag as calcium sources [52, 53]. Several new crystalline phases including CASH, NCASH and $\text{Ca}(\text{OH})_2$ are formed due to slag alkali-activated reactions. The peaks of quartz and illite are almost disappeared indicating a high degree of geopolymerisation. In G_5 , a reduced intensity of the amorphous hump ($2\theta = 25-35$), associated with the formation of thomsonite CASH type gels is observed. The formation of CASH in the matrix forms a basic skeleton of percolating solids which determine the time for the onset of hardening. This quick hardening is not only attributed to CASH formation at an early age but is also due to the higher rate of geopolymerization. Yip *et al.* reported that the presence of calcium leads to precipitate CASH which acts as nucleation sites, and promotes the quick formation of geopolymer gel [54]. Yip's hypothesis also reported that the formation of $\text{Ca}(\text{OH})_2$ could potentially work as a nucleation site for geopolymer formation [55, 56]. The formation of CASH also consumes water and consequently increases the alkalinity of system and further encourages the dissolution of MK particles [57]. This process raises the rate of poly condensation and aluminum silicate geopolymer formation. In G_7 , XRD pattern indicates the formation of Garronite (NCASH) and $\text{Ca}(\text{OH})_2$ phases with geopolymer. Garronite (NCASH) has also previously been detected in alkali-activated slag/metakaolin geopolymers produced from strong activator concentration [58, 59]. Garronite is consequently formed due to the transformation of gismondine; a highly calcium-rich member of zeolite family, to garronite *via* sodium-calcium ion exchange process in high concentrated alkaline medium [59, 60]. It is also probable that $\text{Ca}(\text{OH})_2$ being precipitated from the high alkalinity medium once the presence of soluble Ca ions at the early dissolution step [61]. In G_{10} , XRD show that the main phases are CSH and $\text{Ca}(\text{OH})_2$ with low intensity. Once the Ca ions are dissolved from the starting materials (slag), they prefer to react with silicon ions to yield CSH which are rich in alkalis [62, 63]. The formation of CSH is favored rather than $\text{Ca}(\text{OH})_2$ due to its lower solubility [64].

3.3.3. FTIR of Geopolymers

FTIR spectra of G , G_3 , G_5 , G_7 and G_{10} geopolymers cured for 28 days are shown in Fig. (9). Significant broad bands of OH stretching and bending are observed in the range of 3430-3450 and 1650 cm^{-1} . These are corresponding to adsorbed or cached water molecules in the large voids of polymeric skeleton allied with the reaction products [65, 66]. In FTIR spectra of G_3 , G_5 , G_7 and G_{10} , the bands located between 1420 and 1450 cm^{-1} are assigned to stretching vibrations of O-C-O bond indicating the existence of carbonate which is occurred due to atmospheric carbonation [67]. The presence of higher sodium carbonate content might interrupt the polymerization progression. Increasing contents of BFS also leads to the growth of the carbonate band at 1420 cm^{-1} . The major band between 958 and 1023 cm^{-1} is attributed to asymmetric stretching vibration of Si-O-T bands, where T is tetrahedral silicon or aluminum. The band at about 1065 cm^{-1} Fig. (3) FTIR of metakaolin) corresponding to the Si-O asymmetric stretching in tetrahedral, is shifted to lower wave numbers (about 995-1023 cm^{-1} for G_7 -G) after polymerization reaction as presented in Fig. (9). The shift indicates formation of new highly cross linked geopolymer gel frameworks. The great shift towards lower wave numbers might be due to the partial substitution of SiO_4 tetrahedral by AlO_4 tetrahedral, tend to change in the local chemical surroundings of Si-O bond and newly formed aluminosilicate type gels. The strong shoulder peak for pure MK (seen in Fig. (3) located at 807 cm^{-1} that corresponds to Al-O and Si-O bending, moved to a higher frequency at 870 cm^{-1} after geopolymerization. This is an evidence for the presence of the larger amount of tetrahedral coordinated AlO_4 , formed by dissolution of MK [68, 69]. In G - G_5 , the band at 715 cm^{-1} is attributed to symmetric stretching vibrations of Si-O-Si(Al) bridges, while the bands at 553 and 470 cm^{-1} are ascribed to the symmetric stretching of Al-O-Si and to the bending of Si-O-Si and O-Si-O bonds [70], respectively. This shift to lower wavenumber points out the high level of replacement of Al instead of Si in tetrahedral. In previous works [71, 72], it is indicated that the formation of MK geopolymer in the presence of calcium supports the simultaneous development of cementitious gels C(A)SH and NASH type gels and decreasing the formation of geopolymeric gel [73, 74]. In these systems, Ca^{2+} is supposed to be coupled with the Si-O-Al framework of geopolymeric gel, participating in balancing of negative charge allied with tetrahedral Al (III) and replacing the alkali cations [75, 76]. This is consistent with the move of symmetric stretching vibrations of Si-O-(Si, Al) bridges to higher wavenumber (from 644 to 715 cm^{-1}) with the increase of BFS, which implies the amendment of aluminosilicate structure compared with MK based geopolymers as a sequence of cation replacement in the non-framework sites [77]. This result confirms well with the result of XRD (Fig. 8).

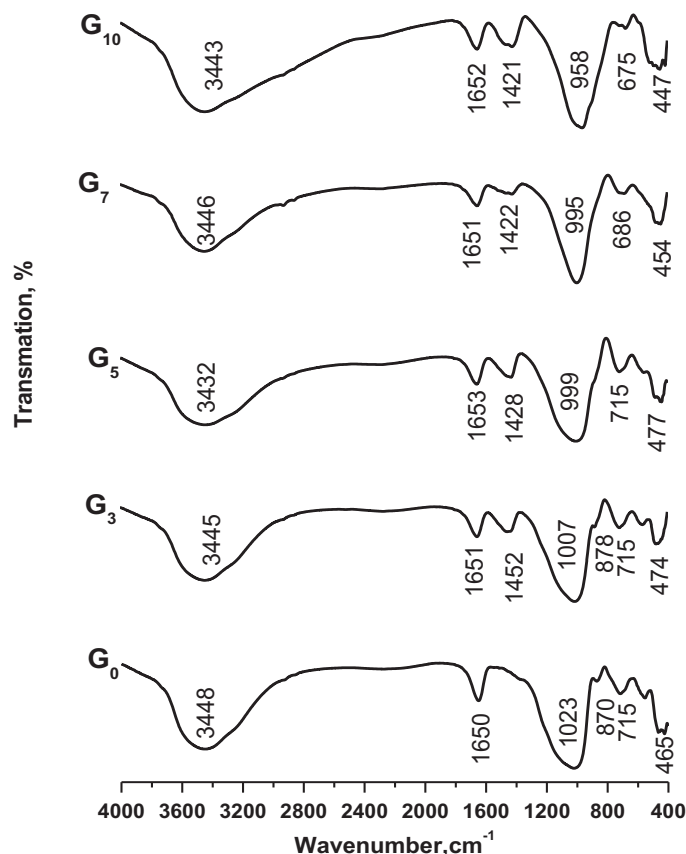


Fig. (9). FTIR spectrum of G, G₃, G₅, G₇ and G₁₀ geopolymers cured for 28 days.

3.3.4. SEM of Geopolymers

SEM was used to analyze the morphology of starting material (MK) and microstructure of G and G₇ geopolymers cured at 28 days. SEM micrographs of MK indicate that the platelet hexagonal structure of kaolinite crystals are relatively disappeared and transferred to relatively amorphous structure with agglomeration due to calcination process at 850°C as shown in Fig. (10). The detected crystals are related to quartz and illite. Some of the particles are within the range of nano size.

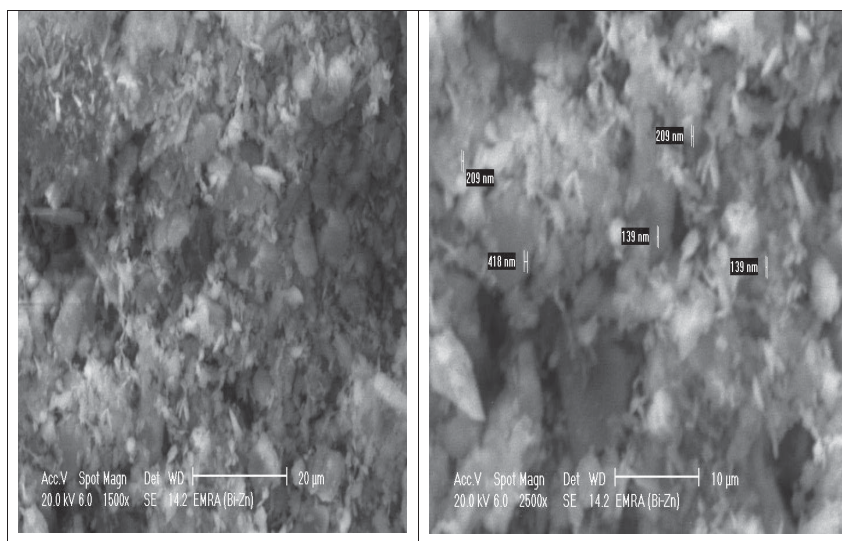


Fig. (10). SEM images of starting materials.

Figs. (11 and 12) show SEM micrographs with EDAX analyses of G and G₇, respectively. Remarkable differences in microstructure are observed for both samples. G₀ exhibits gel-like microstructure produced from geopolymer formation, with some flake-like layer structures similar to that of metakaolinite particulates. It is well known that the solid liquid reaction recognized a gel system with lower water amount, so it is logical to assume that the raw materials can keep their shape during the geopolymerization and molding processes. This is supported by SEM images shown in Fig. (11), which affords extra confirmation to the supposition that geopolymeric reaction is mainly occurred on the surface layer of the solid particulates [78, 79]. This interesting result suggests that the structure of geopolymer maintained partially the sheet of metakaolin after reaction. This crystalline phase can also arise from impurities in raw materials or the process of recrystallization. EDAX analysis of G indicates the presence of Al, Si and O as the main component of the formed geopolymer.

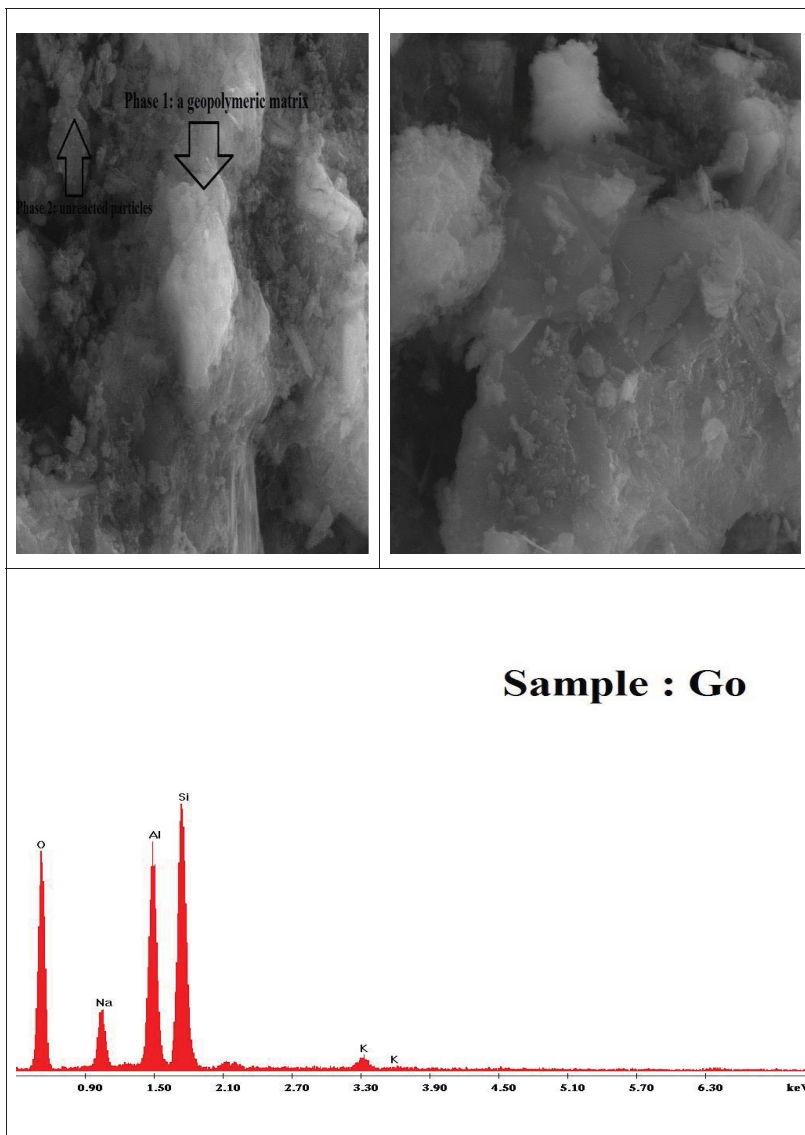


Fig. (11). SEM images and EDAX analysis of G₀ geopolymer.

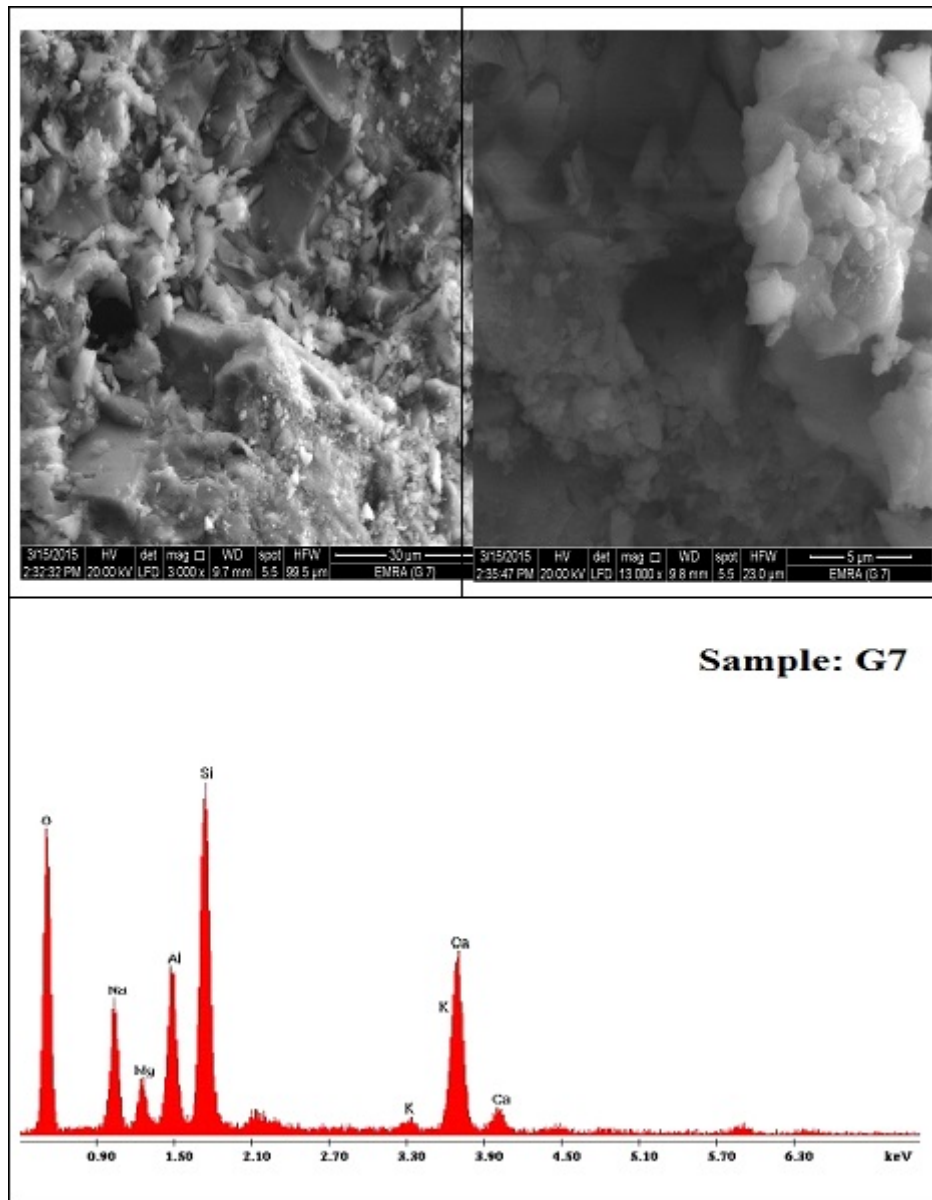


Fig. (12). SEM images and EDAX analysis of G₇ geopolimer.

Fig. (12) shows SEM images and EDAX analysis of G₇ geopolimer. Two individual phases are formed as a result of alkali activation of metakaolin in the presence of BFS *i.e.* geopolymeric gel, (C-A-S-H) gel and some remaining unreacted precursor. Metakaolin particle morphology doesn't vary obviously, but it is linked by a gel-like network. The occurrence of slag promotes connected gel-like structure geopolimer formation. This different feature of microstructure explains the higher hardening rate of G₇ as compared with G. At the early stage of reaction, as the calcium dissolves, CASH is formed in the microstructure. This phase can act as nucleation spot for geopolymerization, rising an intermixed microstructure of CASH and NASH at an early age [80, 81]. The Ca/Si ratio of the CASH formed gel (ca. 0.49) is lower than that Portland cement (1.2 to 2.3). EDAX analysis of this sample indicates the presence of Al, Si, Ca, Na, Mg and O as the component of the predicted phases. Quantitative analysis of G₀ and G₇ are presented in Table [82].

In sample G₇, the ratio of Na/Al is 1.21, and Si/Al ratio is 2.21. Thus, the main geopolymeric gel is inferred to be (Na)-poly(sialate-siloxo-), *i.e.* Na_n-(-Si-O-Al-O-Si-O-)_n-, PSS type. On the other hand, the Na/Al ratio in G system is slightly <1, which points out that only Na⁺ as cation is not enough, so a partial calcium participant in geopolymerization is needed to obtain charge balance [83].

CONCLUSION

The following remarks are concluded:

- The addition of calcium-rich BFS into MK based geopolymers causes properties improvement and shorting in setting time by forming C-A-S-H gel in addition to N-A-S-H gel. Calcium-rich BFS accelerates the hardening process and decreases the alkaline liquid consistency.
- With increasing BFS content, the bulk density increases from 1.67- 2.33g/cm³. Moreover, the bulk density increases with increasing curing time. This is due to the occurring of different chemical reactions which lead to different products and improvement of compressive strength.
- The prepared geopolymers contain two or three phases depending on whether BFS is added or not. For geopolymer with no BFS (G0), it contains two phases, namely; un-reacted metakaolin and geopolymer gel. For geopolymers with CaO sourced from BFS (G1-G10), three phases are formed, namely; un-reacted metakaolin, geopolymer gel and CASH gel.
- The optimum properties were achieved with mix containing 70% slag, after which the deterioration in properties was recorded.

CONSENT FOR PUBLICATION

Not applicable.

CONFLICT OF INTEREST

The authors declare no conflict of interest, financial or otherwise.

ACKNOWLEDGEMENTS

Declared none.

REFERENCES

- [1] Davidovits J. Geopolymers: Inorganic polymeric new materials. *J Therm Anal* 1991; 37: 1633-56. [<http://dx.doi.org/10.1007/BF01912193>]
- [2] Duxson P, Fernandez-Jimenez A, Provis JL, *et al.* Geopolymer technology: The current state of the art. *J Mater Sci* 2007; 42(9): 2917-33. [<http://dx.doi.org/10.1007/s10853-006-0637-z>]
- [3] Duxson P, Lukey GC, Separovic F, van Deventer JSJ. Effect of alkali cations on aluminum incorporation in geopolymeric gels. *Ind Eng Chem Res* 2005; 44(4): 832-9. [<http://dx.doi.org/10.1021/ie0494216>]
- [4] Krivenko PV. Proceedings of the first international conference on alkalineCements and concretes. Kiev, Ukraine: VIPOL Stock Company 1994; pp. 11-129.
- [5] Davidovits J. US Patent 4. 1982; pp. 349-86.
- [6] Hos JP, McCormick PG, Byrne LT. Investigation of a synthetic aluminosilicate inorganic polymer. *J Mater Sci* 2002; 37: 2311-6. [<http://dx.doi.org/10.1023/A:1015329619089>]
- [7] Allahverdi A, Mehrpour K, Kani EN. Taftan Pozzolan-Based Geopolymer Cement. *J Eng Sci* 2008; 19: 1-5.
- [8] Xu H, van Deventer JSJ. Geopolymerisation of multiple minerals. *Miner Eng* 2002; 15: 1131-9. [[http://dx.doi.org/10.1016/S0892-6875\(02\)00255-8](http://dx.doi.org/10.1016/S0892-6875(02)00255-8)]
- [9] Kriven WM, Bell JL, Gordon M. Geopolymer refractories for the glass manufacturing industry. *Ceram Eng Sci Proc* 2004; 25(24): 57-79. [<http://dx.doi.org/10.1002/9780470294857.ch5>]
- [10] Lancellotti I, Kamseu E, Michelazzi M, Barbieri L, Corradi A, Leonelli C. Chemical stability of geopolymers containing municipal solid waste incinerator fly ash. *Waste Manag* 2010; 30(25): 673-79. [<http://dx.doi.org/10.1016/j.wasman.2009.09.032>]
- [11] Andini S, Cioffi R, Colangelo F, Ferone C, Montagnaro F, Santoro L. Characterization of geopolymer materials containing MSWI fly ash and coal fly ash. *Adv Sci Technol* 2010; 69(26): 123-8. [<http://dx.doi.org/10.4028/www.scientific.net/AST.69.123>]
- [12] Giancaspro JW, Papakonstantinou CG, Balaguru P. Flexural response of inorganic hybrid composites with E-glass and carbon fibers. *J Eng Mater Technol* 2010; 132(27): 1-8.
- [13] Ferone C, Colangelo F, Cioffi R, Montagnaro F, Santoro L. Mechanical performances of weathered coal fly ash based geopolymer bricks. *Procedia Eng* 2011; 21: 745-52.

- [http://dx.doi.org/10.1016/j.proeng.2011.11.2073]
- [14] Van Deventer JSJ, Provis JL, Duxson P. Technical and commercial progress in the adoption of geopolymer cement. *Miner Eng* 2012; 29: 89-104.
[http://dx.doi.org/10.1016/j.mineng.2011.09.009]
- [15] Davidovits J. Geopolymer, chemistry and applications, 3rd printing. In: Saint-Quentin, France: Institut Geopolymer 2008.
- [16] Konstantinos AK. Potential of geopolymer technology towards green buildings and sustainable cities. *Procedia Eng* 2011; 21: 1023-32.
[http://dx.doi.org/10.1016/j.proeng.2011.11.2108]
- [17] Davidovits J. Geopolymers-inorganic polymeric new materials. *J Therm Anal* 1991; 37: 1633-56.
[http://dx.doi.org/10.1007/BF01912193]
- [18] Tchakoute Kouamo H, Elimbi A, Mbey JA, Ngally Sabouang CJ, Njopwouo D. The effect of adding alumina-oxide to metakaolin and volcanic ash on geopolymer products: A comparative study. *Constr Build Mater* 2012; 35: 960-9.
[http://dx.doi.org/10.1016/j.conbuildmat.2012.04.023]
- [19] Yip CK, Lukey GC, van Deventer JSJ. Effect of Blast Furnace Slag Addition on Microstructure and Properties of Metakaolinite Geopolymeric Materials. In: Bansal NP, Singh JP, Kriven WM, Schneider H, Ed. *Advances in Ceramic Matrix Composites IX*. Wiley: USA 2003; pp. 187-211.
- [20] Liew YM, Kamarudin H, Mustafa Al Bakri AM, *et al.* Processing and characterization of calcined kaolin cement powder. *Constr Build Mater* 2012; 30: 794-802.
[http://dx.doi.org/10.1016/j.conbuildmat.2011.12.079]
- [21] Boonserm K, Sata V, Pimraksa K, Chindaprasirt P. Improved geopolymerization of bottom ash by incorporating fly ash and using waste gypsum as additive. *Cement Concr Compos* 2012; 34: 819-24.
[http://dx.doi.org/10.1016/j.cemconcomp.2012.04.001]
- [22] Suwan T, Fan M. Influence of OPC replacement and manufacturing procedures on the properties of self-cured geopolymer. *Constr Build Mater* 2014; 73: 551-61.
[http://dx.doi.org/10.1016/j.conbuildmat.2014.09.065]
- [23] Suwan T, Fan M. Influence of OPC replacement and manufacturing procedures on the properties of self-cured geopolymer. *Constr Build Mater* 2014; 73: 551-61.
[http://dx.doi.org/10.1016/j.conbuildmat.2014.09.065]
- [24] Stutzman P. Guide for X-Ray Powder Diffraction Analysis of Portland Cement and Clinker. NISTIR 1996.
- [25] Struble L. The effects of water on maleic and salicylic acid extraction. *Cem and Con Res* 1985; 15(4): 631-6.
- [26] Database M. Mineralogy Database Available from: <http://www.webmineral.com/data/Kaolinite.shtml>
- [27] Bhaskar J, Saikia, gopalakrishnarao parthasarathy, fourier transform infrared spectroscopic characterization of kaolinite from assam and meghalaya, northeastern India. *J Mod Phys* 2010; 1: 206-10.
[http://dx.doi.org/10.4236/jmp.2010.14031]
- [28] Valeria FFB, MacKenzie KJD, Thaumaturgo C. Synthesis and characterisation of materials based on inorganic polymers of alumina and silica: sodium polysialate polymers. *Int J Inorg Mater* 2000; (2): 309-17.
- [29] Farmer VC. The infrared spectra of minerals Mineralogical Society Monogram 4, London (1974), 331.
[http://dx.doi.org/10.1180/mono-4]
- [30] Bernal SA, Provis JL, Rose V, Mejía de Gutierrez R. Evolution of binder structure in sodium silicate-activated slag metakaolin blends. *Cement Concr Compos* 2011; 33(1): 46-54.
[http://dx.doi.org/10.1016/j.cemconcomp.2010.09.004]
- [31] Xu H, Gong W, Larry S, Kevin I, Werner L, Ian L.P. Effect of blast furnace slag grades on fly ash based geopolymer waste forms. *Fuel* 2014; 133: 332-40.
[http://dx.doi.org/10.1016/j.fuel.2014.05.018]
- [32] Phoo-ngernkham T, Chindaprasirt P, Sata V, Hanjitsuwan S, Hatanaka S. The effect of adding nano-SiO₂ and nano-Al₂O₃ on properties of high calcium fly ash geopolymer cured at ambient temperature. *Mater Des* 2014; 55: 58-65.
[http://dx.doi.org/10.1016/j.matdes.2013.09.049]
- [33] Chindaprasirt P, Rattanasak U. Utilization of blended Fluidized Bed Combustion (FBC) ash and Pulverized Coal Combustion (PCC) fly ash in geopolymer. *Waste Manag* 2010; 30(4): 667-72.
[http://dx.doi.org/10.1016/j.wasman.2009.09.040] [PMID: 19854038]
- [34] Chindaprasirt P, Chareerat T, Hatanaka S. CaO T. High-strength geopolymer using fine high-calcium fly ash. *J Mater Civ Eng* 2011; 23: 264-70.
[http://dx.doi.org/10.1061/(ASCE)MT.1943-5533.0000161]
- [35] Xu H, Gong W, Gong W, *et al.* Effect of blast furnace slag grades on fly ash based geopolymer waste forms. *Fuel* 2014; 133: 332-40.
[http://dx.doi.org/10.1016/j.fuel.2014.05.018]
- [36] Bernal SA, Provis JL, Walkley B, *et al.* Gel nanostructure in alkali-activated binders based on slag and fly ash, and effects of accelerated carbonation. *Cement Concr Res* 2013; 53: 127-44.

- [http://dx.doi.org/10.1016/j.cemconres.2013.06.007]
- [37] Ismail I, Bernal SA, Provis JL, San Nicolas R, Hamdan S, van Deventer JSJ. Modification of phase evolution in alkali-activated blast furnace slag by the incorporation of fly ash. *Cement Concr Compos* 2014; 45: 125-35.
[http://dx.doi.org/10.1016/j.cemconcomp.2013.09.006]
- [38] Kumar S, Kumar R, Mehrotra SP. Influence of granulated blast furnace slag on the reaction, structure and properties of fly ash based geopolymer. *J Mater Sci* 2010; 45: 607-15.
[http://dx.doi.org/10.1007/s10853-009-3934-5]
- [39] Susan A, Bernal Erich D, Ruby Mejía de Gutiérrez, Susan A, Provis John L. Mechanical and thermal characterisation of geopolymers based on silicate-activated metakaolin/slag blends. *J Mater Sci* 2011; 46: 5477-86.
[http://dx.doi.org/10.1007/s10853-011-5490-z]
- [40] J. Davidovits, Properties of Geopolymer Cements. In: Krivenko P.V. (Ed.), Proceedings of First International Conference on Alkaline Cements and Concretes, Kiev, Ukraine, 1, 1994, pp. 131-149.].
- [41] Li C, Sun H, Li L. A review: The comparison between alkali-activated slag (Si+Ca) and metakaolin (Si+Al) cements. *Cement Concr Res* 2010; 40: 1341-9.
[http://dx.doi.org/10.1016/j.cemconres.2010.03.020]
- [42] Yip CK, Van Deventer JSJ. Effect of granulated blast furnace slag on geopolymerisation. CD-ROM Proceedings of 6th World Congress of Chemical Engineering. Melbourne, Australia. 2001.
- [43] Rattanasak U, Pankhet K, Chindaprasirt P. Effect of chemical admixtures on properties of high-calcium fly ash geopolymer. *Int J Miner Metall Mater* 2011; 18(3): 364-9.
[http://dx.doi.org/10.1007/s12613-011-0448-3]
- [44] Granizo ML, Alonso S, Blanco-Varela MT, Palomo A. Alkaline Activation of Metakaolin: Effect of Calcium Hydroxide in the Products of Reaction. *J Am Ceram Soc* 2002; 85: 225.
[http://dx.doi.org/10.1111/j.1151-2916.2002.tb00070.x]
- [45] Mackenzie KJD, Komphanchai S, Vagana R. Formation of inorganic polymers (geopolymers) from 2:1 layer lattice aluminosilicates. *J Eur Ceram Soc* 2008; 28: 177.
[http://dx.doi.org/10.1016/j.jeurceramsoc.2007.06.004]
- [46] De Silva P, Sagoe-Crenstil K, Sirivivatnanon V. Kinetics of geopolymerization: Role of Al_2O_3 and SiO_2 . *Cement Concr Res* 2007; 37: 512.
[http://dx.doi.org/10.1016/j.cemconres.2007.01.003]
- [47] Bell JL, Sarin P, Driemeyer PE, *et al.* X-ray pair distribution function analysis of a metakaolin-based, $KAlSi_2O_6 \cdot 5.5H_2O$ inorganic polymer (geopolymer). *J Mater Chem* 2008; 18: 5974-81.
[http://dx.doi.org/10.1039/b808157c]
- [48] Zawrah MF, S. Farag Rabei, Kohail MH. Improvement of physical and mechanical properties of geopolymer through addition of zircon, *Materials Chemistry and Physics*. 15 September 2018; 217.
[http://dx.doi.org/10.1016/j.matchemphys.2018.06.024]
- [49] Granizo ML, Blanco MT, Puertas F, Palomo A. Alkaline activation of metakaolin: Influence of synthesis parameters, Proceeding of the Tenth International Congress on Chemistry of Cement. Göteborg 1997; 3.
- [50] Granizo ML, Alonso S, Blanco-Varela MT, Palomo A. Alkaline activation of metakaolin: Effect of calcium hydroxide in the products of reaction. *J Am Ceram Soc* 2002; 85(1): 225-31.
[http://dx.doi.org/10.1111/j.1151-2916.2002.tb00070.x]
- [51] Pacheco-Torgal F, Castro-Gomes J, Jalali S. Alkali-activated binders: A review. Part 1. Historical background, terminology, reaction mechanisms and hydration products. *Constr Build Mater* 2008; 22: 1305-14.
[http://dx.doi.org/10.1016/j.conbuildmat.2007.10.015]
- [52] Pacheco-Torgal F, Castro-Gomes J, Jalali S. Alkali-activated binders: A review. Part 1. Historical background, terminology, reaction mechanisms and hydration products. *Constr Build Mater* 2008; 22: 1305-14.
[http://dx.doi.org/10.1016/j.conbuildmat.2007.10.015]
- [53] Yip CK, van Deventer JSJ. Microanalysis of calcium silicate hydrate gel formed within a geopolymeric binder. *J Mater Sci* 2003; 38(18): 3851-60.
[http://dx.doi.org/10.1023/A:1025904905176]
- [54] Christina K, Yip Grant C, Lukey John L, *et al.* Effect of calcium silicate sources on geopolymerisation. *Cement Concr Res* 2008; 38: 554-64.
[http://dx.doi.org/10.1016/j.cemconres.2007.11.001]
- [55] Yip CK, Lukey GC, van Deventer JSJ. The coexistence of geopolymeric gel and calcium silicate hydrate at the early stage of alkaline activation. *Cement Concr Res* 2005; 35: 1688-97.
[http://dx.doi.org/10.1016/j.cemconres.2004.10.042]
- [56] Zhang YJ, Wang YC, Xu DL, Li S. Mechanical performance and hydration mechanism of geopolymer composite reinforced by resin. *Mater Sci Eng A* 2010; 527(24-25): 6574-80.
[http://dx.doi.org/10.1016/j.msea.2010.06.069]

- [57] Bernal SA, Provis JL, Rose V, Mejía de Gutiérrez R. High-resolution X-ray diffraction and fluorescence microscopy characterization of alkali-activated slag-metakaolin binders. *J Am Ceram Soc* 2013; 96(6): 1951-7. [<http://dx.doi.org/10.1111/jace.12247>]
- [58] Ismail I, Bernal SA, Provis JL, San Nicolas R, Hamdan S, van Deventer JSJ. Modification of phase evolution in alkali-activated blast furnace slag by the incorporation of fly ash. *Cement Concr Compos* 2014; 45: 125-35. [<http://dx.doi.org/10.1016/j.cemconcomp.2013.09.006>]
- [59] Zhang YJ, Wang YC, Xu DL, Li S. Mechanical performance and hydration mechanism of geopolymer composite reinforced by resin. *Mater Sci Eng A* 2010; 527: 6574-80. [<http://dx.doi.org/10.1016/j.msea.2010.06.069>]
- [60] Bernal SA, Provis JL, Rose V, Mejía de Gutiérrez R. Evolution of binder structure in sodium silicate-activated slag-metakaolin blends. *Cement Concr Compos* 2011; 33(1): 46-54. [<http://dx.doi.org/10.1016/j.cemconcomp.2010.09.004>]
- [61] Yip CK, van Deventer JSJ. Microanalysis of calcium silicate hydrate gel formed within a geopolymeric binder. *J Mater Sci* 2003; 38(18): 3851-60. [<http://dx.doi.org/10.1023/A:1025904905176>]
- [62] Shi C, Krivenko PV, Roy DM. *Alkali-Activated Cements and Concretes*. Abingdon, UK: Taylor and Francis 2006. [<http://dx.doi.org/10.4324/9780203390672>]
- [63] García-Lodeiro I, Palomo A, Fernández-Jiménez A, Macphee DE. Compatibility studies between N-A-S-H and C-A-S-H Gels. Study in the ternary diagram $\text{Na}_2\text{O}-\text{CaO}-\text{Al}_2\text{O}_3-\text{SiO}_2-\text{H}_2\text{O}$. *Cement Concr Res* 2011; 41(2): 923-31. [<http://dx.doi.org/10.1016/j.cemconres.2011.05.006>]
- [64] Lloyd RR, Provis JL, van Deventer JSJ. Microscopy and microanalysis of inorganic polymer cements 2: The gel binder. *J Mater Sci* 2009; 44(2): 620-31. [<http://dx.doi.org/10.1007/s10853-008-3078-z>]
- [65] Temuujin J, van Riessen A, Williams R. Influence of calcium compounds on the mechanical properties of fly ash geopolymer pastes. *J Hazard Mater* 2009; 167(1-3): 82-8. [<http://dx.doi.org/10.1016/j.jhazmat.2008.12.121>] [PMID: 19201089]
- [66] García-Lodeiro I, Fernández-Jiménez A, Palomo A, Macphee DE. Effect of calcium additions on N-A-S-H cementitious gels. *J Am Ceram Soc* 2010; 93(7): 1934-40.
- [67] Puligilla S, Mondal P. Role of slag in microstructural development and hardening of fly ash-slag geopolymer. *Cement Concr Res* 2013; 43: 70-80. [<http://dx.doi.org/10.1016/j.cemconres.2012.10.004>]
- [68] Ben Haha M, Lothenbach B, Le Saout G, Winnefeld F. Influence of slag chemistry on the hydration of alkali-activated blast-furnace slag — Part II: Effect of Al_2O_3 . *Cement Concr Res* 2012; 42: 74-83. [<http://dx.doi.org/10.1016/j.cemconres.2011.08.005>]
- [69] Zawrah MF, Khattab RM, Saad EM, Gado RA. Effect of Surfactant Types and Their Concentration on the Structural Characteristics of Nanoclay. *Spectrochimica Acta, Part A: Molecular and Biomolecular Spectroscopy* 2014; 122: 616-23. [<http://dx.doi.org/10.1016/j.saa.2013.11.076>]
- [70] Lecomte I, Henrist C, Liegeois M, Maseri F, Rulmont A, Cloots R. (Micro)-structural comparison between geopolymers, alkali-activated slag cement and Portland cement. *J Eur Ceram Soc* 2006; 26: 3789-97. [<http://dx.doi.org/10.1016/j.jeurceramsoc.2005.12.021>]
- [71] Lee WKW, van Deventer JSJ. Use of infrared spectroscopy to study geopolymerization of heterogeneous amorphous aluminosilicates. *Langmuir* 2003; 19(21): 8726-34. [<http://dx.doi.org/10.1021/la026127e>]
- [72] Alonso S, Palomo A. Alkali activation of metakaolin and calcium hydroxide mixtures: Influence of temperature, activator concentration and solids ratio. *Mater Lett* 2001; 47(2): 55-62. [[http://dx.doi.org/10.1016/S0167-577X\(00\)00212-3](http://dx.doi.org/10.1016/S0167-577X(00)00212-3)]
- [73] Bernal SA, Provis JL, Rose V, Mejía de Gutiérrez R. Evolution of binder structure in sodium silicate-activated slag-metakaolin blends. *Cement Concr Compos* 2011; 33(1): 46-54. [<http://dx.doi.org/10.1016/j.cemconcomp.2010.09.004>]
- [74] Bernal SA, Rodríguez ED, Mejía de Gutiérrez R, Gordillo M, Provis JL. Mechanical and thermal characterization of geopolymers based on silicate-activated metakaolin/slag blends. *J Mater Sci* 2011; 46(16): 5477-86. [<http://dx.doi.org/10.1007/s10853-011-5490-z>]
- [75] García-Lodeiro I, Macphee DE, Palomo A, Fernández J. Effect of alkalis on fresh C-S-H gels. FTIR analysis. *Cement Concr Res* 2009; 39: 147-53. [<http://dx.doi.org/10.1016/j.cemconres.2009.01.003>]
- [76] García-Lodeiro I, Fernández Jiménez A, Palomo A, Macphee DE. Effect on fresh C-S-H gels of simultaneous addition of alkali and aluminum. *Cement Concr Res* 2010; 40: 27-32. [<http://dx.doi.org/10.1016/j.cemconres.2009.08.004>]

- [77] Provis JL, Yong SL, Duxson P, van Deventer JSJ. Geopolymer structures and kinetics: What have we learnt lately? 3rd International Symposium on Non-Traditional Cement and Concrete. Brno, Czech Republic. 2008; pp. 589-97.
- [78] Susan A Bernal, Erich D Rodríguez, Gutiérrez Ruby Mejía de, Provis John L, Delvasto Provis Silvio. Activation of Metakaolin/Slag Blends Using Alkaline Solutions Based on Chemically Modified Silica Fume and Rice Husk Ash, Waste Biomass Valor [http://dx.doi.org/10.1016/S1466-6049(00)00041-6]
- [79] Valeria FFB, Kenneth JDM, Clelio T. Synthesis and characterization of materials based on inorganic polymers of alumina and silica: Sodium polysialate polymers. *Int J Inorg Mater* 2000; 2: 309-17. [http://dx.doi.org/10.1016/S1466-6049(00)00041-6]
- [80] Wang RH, Li H, Yan F. Synthesis and mechanical properties of metakaolinite-based geopolymer. *Colloids Surf A Physicochem Eng Asp* 2005; 268: 1-6. [http://dx.doi.org/10.1016/j.colsurfa.2005.01.016]
- [81] Zawrah MF, Gado RA, Feltin N, Ducourtieux S, Devoille L. Recycling and utilization assessment of waste fired clay bricks (Grog) with granulated blast-furnace slag for geopolymer production. *Process Saf Environ Prot* 2016; 103: 237-51. [http://dx.doi.org/10.1016/j.psep.2016.08.001]
- [82] Puligilla S, Mondal P. Role of slag in microstructural development and hardening of fly ash-slag geopolymer. *Cement Concr Res* 2013; 43: 70-80. [http://dx.doi.org/10.1016/j.cemconres.2012.10.004]
- [83] Guo X, Shi H, Warren AD. Compressive strength and microstructural characteristics of class C fly ash geopolymer. *Cement Concr Compos* 2010; 32: 142-7. [http://dx.doi.org/10.1016/j.cemconcomp.2009.11.003]

© 2018 Zawrah *et al.*

This is an open access article distributed under the terms of the Creative Commons Attribution 4.0 International Public License (CC-BY 4.0), a copy of which is available at: (<https://creativecommons.org/licenses/by/4.0/legalcode>). This license permits unrestricted use, distribution, and reproduction in any medium, provided the original author and source are credited.